Iron-meditated fungal starvation by lupine rhizosphere-associated and extremotolerant *Streptomyces* sp. S29 desferrioxamine production

Scott A. Jarmusch[a,c]*, Diego Lagos-Susaeta[b]†, Emtinan Diab[a]†, Oriana Salazar[b], Juan A. Asenjo[b], Rainer Ebel[a], Marcel Jaspars[a]*

[a] Marine Biodiscovery Centre, Department of Chemistry, University of Aberdeen, Old Aberdeen AB24 3UE, Scotland, U.K.

[b] Centre for Biotechnology and Bioengineering, University of Chile, Beauchef 850, Santiago, Chile.

[c] Department of Pharmaceutical Biosciences – Pharmacognosy, Uppsala University, Biomedicinskt Centrum, Uppsala, Sweden 751 23

†Authors contributed equally to this work

*Corresponding authors: scott.jarmusch@farmbio.uu.se; m.jaspars@abdn.ac.uk

ABSTRACT

Siderophores are iron-chelating compounds that aid iron uptake, one of the key strategies for microorganisms to carve out ecological niches in microbially diverse environments. Desferrioxamines are the principal siderophores produced by *Streptomyces* spp. Their biosynthesis has been well studied and as a consequence, the chemical potential of the pathway continues to expand. With all of this in mind, our study aimed to explore extremotolerant and Lupine rhizosphere-derived *Streptomyces* sp. S29 for its potential antifungal capabilities. Cocultivation of isolate S29 was carried out with *Aspergillus niger* and *Botrytis cinerea*, both costly fungal phytopathogens in the wine industry, to simulate their interaction within the rhizosphere. The results indicate that not only is *Streptomyces* sp. S29 extraordinary at producing hydroxamate siderophores but uses siderophore production as a means to 'starve' the fungi of iron. High resolution LC-MS/MS followed by GNPS molecular networking was used to observe the datasets for desferrioxamines and guided structure elucidation of new desferrioxamine analogues. Comparing the new chemistry, using tools like molecular networking and MS2LDA, with the known biosynthesis, we show that the chemical potential of the desferrioxamine pathway has further room for exploration.

33 **INTRODUCTION**

34 The application of *Streptomyces* secondary metabolites goes beyond drug
35 discovery, as they are one of the most important bacteria for crop protection. Their
36 biotechnological application as rhizosphere or endophytic bacteria is proven to confer
37 protection against soilborne pathogens like fungi, nematodes, and other bacteria.[1,2] They
38 serve as an important factor in 'disease suppressive soils', with several mechanisms of
39 action including synthesis of plant growth regulators[3], antibiotic production[2], secretion of
40 volatile compounds[4], and siderophore production.[5] The last of these is not only a way for
41 bacteria to uptake vital metals from the surrounding soil but also to sequester metals in
42 order to gain a competitive edge against other soilborne organisms.

43 Rhizosphere-associated microbes are one of the many strategies currently being
44 explored as biocontrol agents. Bacterial communities in the rhizosphere contribute to the
45 extremely complex flow of nutrients as well as the export of antibiotics and other
46 secondary metabolites into the soil.[6,7] Model organisms from genera like *Bacillus* and
47 *Pseudomonas* have traditionally been promising sources due to their association to the
48 soil and their production of secondary metabolites like lipopeptides but also plant growth
49 promotors.[8,9] Actinobactera, which are also predominantly soil-associated microbes,
50 have also been explored as biocontrol agents due to their prolific antimicrobial potential.[10]
51 This combined with the fact that extremotolerant microbes have adapted to the harsh
52 conditions and the potential of these adaptations to be translatable to biotechnologies,
53 extremotolerant microbes look to be promising sources as biocontrol agents.[11] In Chile,
54 the wine industry is the main agricultural export, estimated at ~$2 billion USD in 2017[12],

55 thus driving a large research interest around protection of wine-producing grapes against
56 various phytopathogens.

57 Siderophores are iron-chelating compounds that aid metal uptake in iron deficient
58 environments.[13] These secondary metabolites are produced by all microbes and four
59 types of siderophore-mediated social interactions have been observed: uptake among
60 clonal cells (sharing), cheating or piracy (which can only happen amongst microbes with
61 the same uptake receptor), competition via locking away and metabolite competition
62 (whichever microbe makes the most cost efficient and effective chelator).[14]
63 Desferrioxamines (DFO) are the most widely observed group of siderophores in
64 *Streptomyces* spp., used principally for Fe(III) scavenging[13,15], as well as some other
65 heavy metals.[16–18] Since the vast majority of organisms require Fe(III) in order to maintain
66 proper cell wall function[13], as one scavenges for itself, it simultaneously starves other
67 competing organisms, rendering them potentially unviable.

68 The biosynthetic machinery of desferrioxamines has been well studied[19–21] and as
69 a consequence, the chemical potential continues to expand. The substrate specificity of
70 DesC-like proteins, similar to acyl CoA-dependent transferases, seems to be the key
71 factor in producing diverse desferrioxamine scaffolds.[19,21] It has been shown that DesC
72 can accommodate for acetyl, succinyl, and myristol-CoA, with the latter providing insight
73 into the production of acyl desferrioxamines.[19] Additionally, aryl desferrioxamines, first
74 isolated from *Micrococcus luteus* KLE1011[22] and later from *Streptomyces* sp. MA37[23],
75 showed further substrate flexibility, where the latter communication described a new
76 biosynthetic gene cluster (BGC) which contained a DesC homolog (LgoC). This enzyme
77 promiscuity fits ideally with the Screening Hypothesis first proposed by Firn and Jones;

78 secondary metabolism stems from metabolic pathways that 'maximize diversity and
79 minimize cost'.[24]

80 Due to the modular nature of desferrioxamines and the presence of peptide bonds
81 throughout their structure, mass spectrometry-based studies have been utilized
82 extensively to not only study their biological impact but also for elucidation of new
83 structures. Previous studies have established standard fragmentation patterns of these
84 siderophores, even as far as elucidating new structures solely based on mass
85 spectrometry.[25–31] This standardized fragmentation makes the discovery of siderophores
86 much easier thanks to metabolomics-based tools like molecular networking, like Global
87 Natural Products Social Molecular Networking (GNPS). It allows for correlations to be
88 drawn within your dataset and against the GNPS library that relates similar MS/MS
89 spectra to one another, forming clusters or families of similar features.[32]

90 With all of this in mind, our study originally aimed to explore extremotolerant,
91 rhizosphere-derived *Streptomyces* sp. S29, a novel strain, for antifungal secondary
92 metabolites. Cocultivation of S29 with *Aspergillus niger* and *Botrytis cinerea*, both costly
93 fungal phytopathogens in the wine industry, were carried out in a fashion to allow S29 to
94 dominate the culture, thus eliciting a chemical response from the addition of each fungus.
95 Bioassay-guided fractionation lead to no lead compounds as potential antifungal agents
96 yet post-fermentation streaks of inoculum showed no fungal growth. High resolution LC-
97 MS/MS followed by GNPS molecular networking was used to analyse the data sets. The
98 results indicated that not only is *Streptomyces* sp. S29 extraordinary at producing
99 hydroxamate siderophores, totalling 24 new analogues and 8 previously identified ones
100 confirmed through MS/MS structure elucidation, but uses siderophore production as a

101 means to ‘starve’ the fungi of iron. When grown in coculture with the fungi, 22 additional
102 new analogues and 17 additional previously described were identified, clearly showing a
103 chemical response to the fungi in culture environment. Using MS2LDA to further explore
104 desferrioxamine chemical space, we observed that it is potentially 2.5 times larger than
105 previously anticipated. These results point to the potential of *Streptomyces* sp. S29 as a
106 biocontrol agent to prevent fungal infection and the potential for new desferrioxamine
107 chemistry.

RESULTS AND DISCUSSION

***Streptomyces* sp. S29 cocultivation and LC-MS of desferrioxamine-rich fractions.** Preliminary fungal bioassay screening of the lupine rhizosphere *Streptomyces* culture collection showed a novel strain, *Streptomyces* sp. S29, inhibited the growth of *Botrytis cinerea* when grown in coculture on solid medium (Figure 1). In an attempt to induce production of antifungal metabolites, the bacteria and fungi were cocultivated in liquid culture in a fashion to allow for *Streptomyces* sp. to be the dominant microbe. Bioassay guided fractionation of the *sec*-butanol fraction lead to no antifungal leads even though inhibition was observed against *B. cinerea* only (Figure S6). Upon LC-MS and ^{1}H NMR analysis of the extracts, a profusion of DFOs was observed in all *sec*-butanol fractions, leading to the hypothesis that this *Streptomyces* sp. uses a different mechanism than producing antimycotics to combat the fungal cocultivate, as seen previously in human bacterial infections.[33] DFOs historically have never exhibited antimicrobial activity and therefore we confidently presume they are not responsible for the inhibition seen in Figure S6.[34] Time-dependent growth inhibition of *Penicillium* was observed when exposed to varying concentrations of coproporphyrin, a siderophore produced by *Glutamicibacter arilaitensis*[35], but this activity has never been shown for desferrioxamines. *Streptomyces* sp. S29 was also grown in monoculture on iron deficient medium to induce production of DFOs in an attempt to compare siderophore production to the coculture experiments. *Aspergillus niger* and *Botrytis cinerea* were chosen as the fungal phytopathogens due to their established pathology of wine producing grapes [36,37] and the importance of wine as Chile's main agricultural export. Additionally, these fungi would be encountered in

130 *Streptomyces* sp. S29's ecological niche, making this an important evaluation of microbes
131 it would encounter in the soil environment.

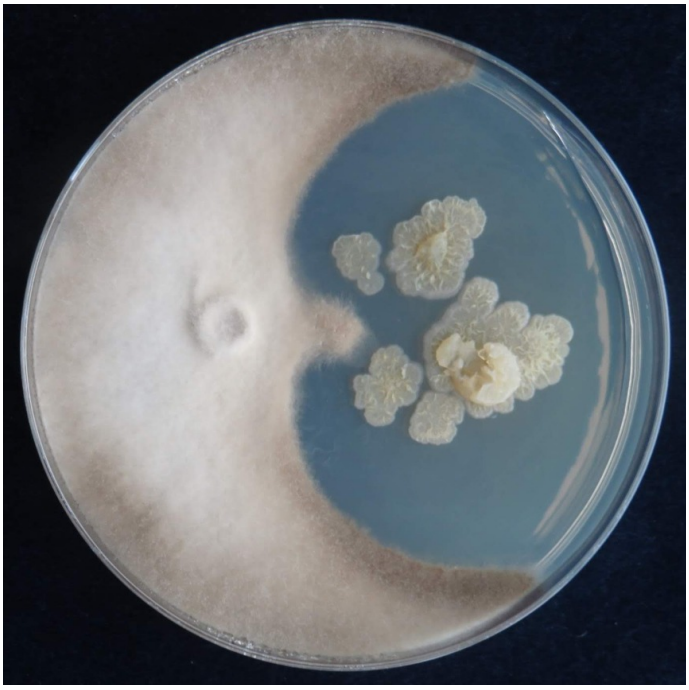

Figure 1. Preliminary antifungal screening on *Streptomyces* isolate S29 (right) grown with *Botrytis cinerea* (left). Image courtesy of Diego Lagos-Susaeta.

132

133 Extracts and fractions were evaluated for the presence of two DFOs (B and D1)
134 during the fractionation steps, in order to trace the fractions that contained the highest
135 abundance of siderophores. Presence of DFOs was further evaluated at the final stages
136 of separation based on the molecular families generated from molecular networking,
137 utilizing the known DFOs in the GNPS library as anchor points, which further aided
138 structure elucidation. Based on the LC-MS results, the butanol partitions contained the
139 largest abundance of DFOs, and therefore this data was used to generate a molecular
140 network using GNPS.

141 **Molecular networking and MS/MS based structure elucidation.** The molecular
142 network generated contained 1169 molecular features after removal of features

143 originating from media and instrument blanks. Each subnetwork was approached using
144 GNPS library hits as ‘anchors’ (hexagons in each subnetwork) and then collecting the
145 masses of linked nodes and predicting molecular formula from the raw data. Using these
146 ‘anchors’ not only allows one to relate the nodes directly connected to the anchor, but
147 also gives broader sense of the molecular nature of a cluster. The hydroxamate
148 siderophores were primarily distributed amongst three principle molecular families
149 (Figures 2-4). Subnetwork 1 (Figure 2) contained a number of new acyl DFO D-like
150 analogues that are first described in this study as well as new analogues of acyl DFO B-
151 like derivatives. Subnetwork 2 (Figure 3) is mostly composed of unknown derivatives
152 although a suite of new macrocyclised DFOs and tenacibactin derivatives, first described
153 by Jang et al. [38], were observed. The last principle subnetwork contained various Fe(III)
154 and Al(III) complexed FOs (Figure 6). Within this network a new analogue was identified,
155 uC_{12} acyl FO-B, while its non-chelated form was not observed in the data (Figure S32).
156 Aryl desferrioxamines related to the previously described acyl ferrioxamine 1 (also
157 known as legonoxamine A) and 2 were also found distributed amongst varying molecular
158 families across the molecular network and do not seem to link into their own cluster such
159 as that seen for the DFO-Ds and DFO-Bs. For the remaining small molecular families that
160 contain DFOs, we observed a group of sodiated adducts, large acyl DFO-Bs, as well as
161 the macrocyclised desferrioxamine E (Figure S1). The remaining nodes that link within
162 the desferrioxamine molecular families were unable to be identified using the annotation
163 workflow described in Figure 4.

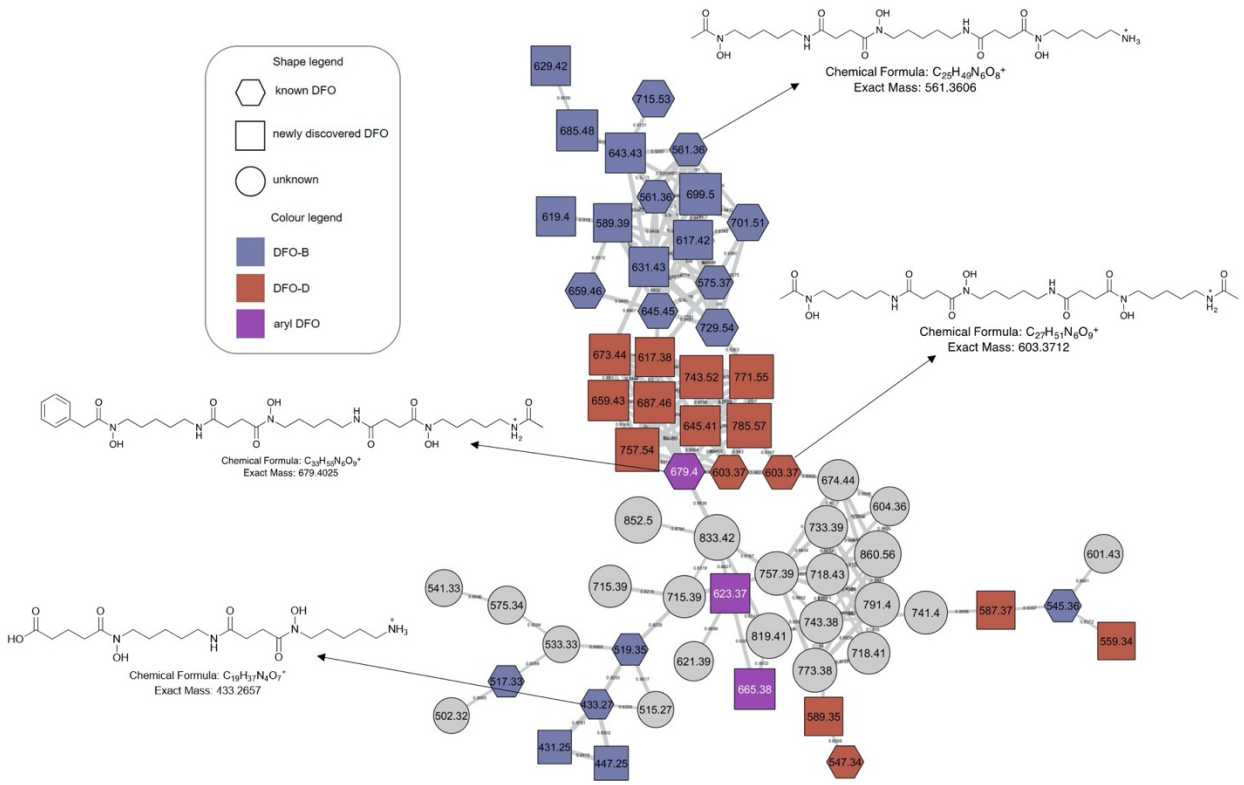

Figure 2. Desferrioxamine subnetwork 1. Distributed amongst the molecular family are DFO-Bs (blue), DFO-Ds (red), and aryl DFOs (purple). Grey nodes represent potential DFOs that were not able to be annotated using MS/MS data only.

164

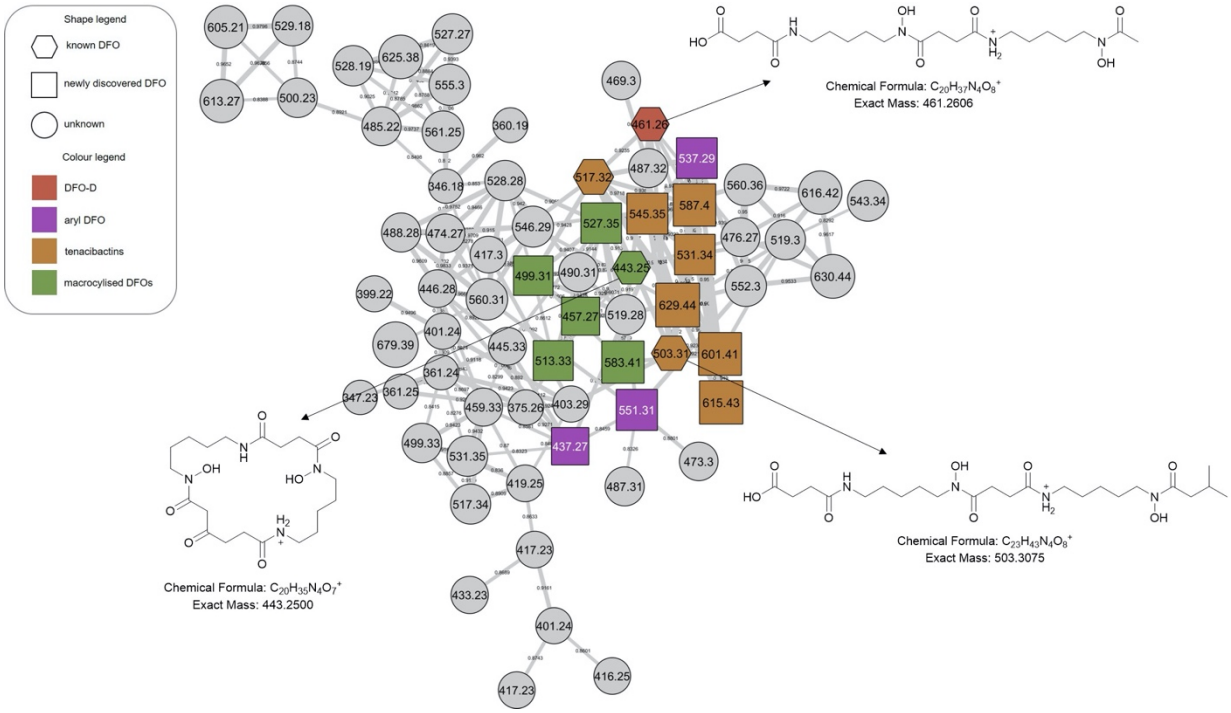

Figure 3. Desferrioxamine subnetwork 2. Within the molecular family are macrocyclised DFOs (green) as well as a number of new tenacibactin derivatives (orange). Grey nodes represent potential DFOs that were not able to be annotated using MS/MS data only.

165

166 MS/MS based structure elucidation was carried out in a similar fashion to studies
167 conducted previously (Figure 4).[25–28] Early observations of desferrioxamine B and D1
168 fragmentation showed an initial loss of the N-terminus, corresponding to the loss of either
169 118.1 or 160.1. Using this as a foundation, structures were either started with a *N*-
170 hydroxycadaverine or a *N*-hydroxy-*N*-acetylcadaverine, respectively. The remainder of
171 structure elucidation was completed stepwise: (1) predicting the molecular formula from
172 the accurate mass and collection of MS/MS data, (2) filling out the structures with
173 appropriate desferrioxamine precursors (i.e. *N*-hydroxycadaverine, putrescine, succinate,
174 acetate, etc.), and (3) taking the remainder of the molecular formula and placing an
175 appropriate acid at the C-terminus that either has precedent from previous studies or
176 could be a potential binding partner with an acyltransferase like coenzyme A.

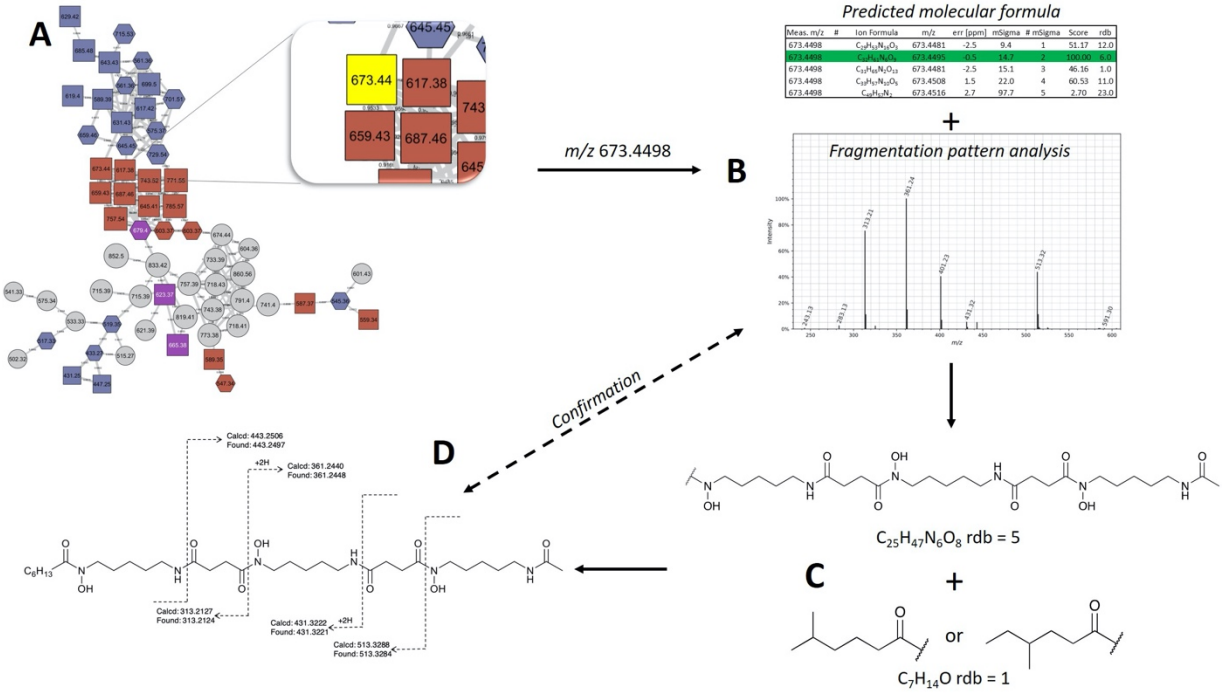

Figure 4. Molecular network and MS/MS based structure determination. (A) molecular networks generated using GNPS were dereplicated and potentially unknown ions were found in the Raw data. (B) Predicted molecular formula were generated and the most likely candidate formula was chosen. MS/MS spectra were analysed for the initial loss of -118 or -160 to determine the N-terminal moiety of *N*-hydroxycadaverine or *N*-acetylhydroxycadaverine, respectively. (C) Based on known structure of desferrioxamines, substructures were proposed for each new metabolite and lastly, (D) putative structures were supported by MS/MS data, although further spectroscopic characterisation would be required for confirmation.

179 Overall, 41 new DFO analogues were identified in the molecular network and
180 through manual data processing (Table 1). These range from short acyl chain DFO-Bs,
181 acyl desferrioxamine D-like (DFO-D) analogues which have not previously been
182 described, tenacibactins, aryl DFOs, and long chain dicarboxylate DFOs (Table 1).
183 Additionally, 5 uncertain macrocyclic and 25 known hydroxamate siderophores were
184 detected, including known acyl, aryl DFOs and bisucaberins, giving further credence to
185 the new structure assignments. Their identification, observed presence in monoculture
186 and/or coculture, and identification confidence based on Schymanski's rules[39] are present
187 in Table 1. Schymanski's rule distinguish various levels of confidence for mass spectral-
188 based assignments, where the highest score is 1 (verifiable by MS, MS^2, RT, and an
189 internal standard) and the lowest score is 5 (exact mass only). The majority of the
190 identified compounds rank at level 2 or level 3 on the Schymanski scale.

Table 1. Summary of siderophores identified using molecular networking and manual observations of the data. Nomenclature that are italicized were identified in this study.

	Name	Measured mass [M+H]+	Theoretical mass [M+H]+	Δ ppm	Sum formula [+H]+	ID confidence	Monoculture	Reference
cyclic desferrioxamines	Bisu-03	429.2344	429.2342	-0.46	$C_{19}H_{33}N_4O_7$	2		Senges et al.
	Bisu-01	443.2495	443.2500	-1.13	$C_{20}H_{35}N_4O_7$	2		Senges et al.
	Uncertain structure	457.2660	457.2657	0.65	$C_{21}H_{37}N_4O_7$	3	*	*This study*
	Uncertain structure	499.3110	499.3126	-3.20	$C_{24}H_{43}N_4O_7$	3	*	*This study*
	Uncertain structure	513.3310	513.3283	5.25	$C_{25}H_{45}N_4O_7$	3	*	*This study*
	Uncertain structure	527.3450	527.3439	2.08	$C_{26}H_{47}N_4O_7$	3	*	*This study*
	Uncertain structure	583.4050	583.4065	-2.57	$C_{30}H_{55}N_4O_7$	3		*This study*
	desferrioxamine E	601.3557	601.3556	0.17	$C_{27}H_{49}N_6O_9$	2		
aryl desferrioxamines	legonoxamine B	337.1754	337.1758	-1.19	$C_{17}H_{25}N_2O_5$	2		Maglangit et al.
	legonoxamine C	351.1912	351.1914	-0.57	$C_{18}H_{37}N_4O_5$	3		*This study*
	legonoxamine D	437.2755	437.2758	-0.69	$C_{22}H_{37}N_4O_5$	3		*This study*
	legonoxamine E	537.2924	537.2919	0.93	$C_{26}H_{41}N_4O_8$	3	*	*This study*
	legonoxamine F	551.3088	551.3075	2.36	$C_{27}H_{43}N_4O_8$	3		*This study*
	legonoxamine G	623.3764	623.3763	0.16	$C_{30}H_{51}N_6O_8$	3	*	*This study*
	acyl-ferrioxamine 1/ legonoxamine A	637.3917	637.3919	-0.31	$C_{31}H_{53}N_6O_8$	2	*	D'Onofrio et al; Maglangit et al.
	legonoxamine H	665.3893	665.3869	3.61	$C_{32}H_{53}N_6O_9$	3		*This study*
	acyl-ferrioxamine 2	679.4025	679.4025	0.00	$C_{33}H_{55}N_6O_9$	2	*	D'Onofrio et al.
	legonoxamine A glycoside	799.4456	799.4448	1.00	$C_{37}H_{63}N_6O_{13}$	3	*	*This study*
DFO-Bs	*un-pre[5+5*]*	431.2500	431.2520	-4.63	$C_{19}H_{35}N_4O_7$	3		*This study*
	pre[5+5*]	433.2662	433.2657	-1.15	$C_{19}H_{37}N_4O_7$	2		Rütschlin et al.
	pre[5+5] aldehyde*	447.2450	447.2449	0.22	$C_{19}H_{35}N_4O_8$	3		*This study*
	pre[ha+5+5*]	517.3221	517.3232	-2.12	$C_{24}H_{45}N_4O_8$	2		Rütschlin et al.
	abloxime / IC202C	517.3347	517.3344	0.58	$C_{23}H_{45}N_6O_7$	2	*	Iijima et al.
	proferrioxamine G1t	519.3495	519.3501	-1.16	$C_{23}H_{47}N_6O_7$	2		Feistner et al.
	DesuA1	545.3658	545.3657	0.18	$C_{25}H_{49}N_6O_7$	2	*	Senges et al.
	DesA1	547.3449	547.3450	-0.18	$C_{24}H_{47}N_6O_8$	2	*	Senges et al.
	Des A2 / IC202B	557.2880	557.2881	-0.18	$C_{23}H_{43}N_6O_8Al$	2		Iijima et al.
	desferrioxamine B	561.3602	561.3606	-0.71	$C_{25}H_{49}N_6O_8$	2	*	
	desferrioxamine N /desf-05	575.3762	575.3763	-0.17	$C_{26}H_{51}N_6O_8$	2	*	Ejje et al; Senges et al.
	C3 acyl DFO-B	589.3915	589.3919	-0.68	$C_{27}H_{53}N_6O_8$	2	*	*This study*
	C4 acyl DFO-B	603.4073	603.4076	-0.49	$C_{28}H_{55}N_6O_8$	2	*	*This study*
	C5 acyl DFO-B	617.4233	617.4232	0.16	$C_{29}H_{57}N_6O_8$	2	*	*This study*
	C4 acyl hydroxylated DFO-B	619.4024	619.4025	-0.16	$C_{29}H_{55}N_6O_9$	3	*	*This study*
	uC6 acyl DFO-B	629.4238	629.4232	0.95	$C_{30}H_{57}N_6O_8$	3		*This study*
	C6 acyl DFO-B	631.4388	631.4389	-0.16	$C_{30}H_{59}N_6O_8$	2	*	*This study*
	uC7 acyl DFO-B	643.4389	643.4389	0.00	$C_{31}H_{59}N_6O_8$	3		*This study*
	C7 acyl-DFO	645.4550	645.4545	0.77	$C_{31}H_{61}N_6O_8$	2		Traxler et al; Sidebottom et al.
	C8 acyl-DFO	659.4697	659.4702	-0.76	$C_{32}H_{63}N_6O_8$	2		Traxler et al; Sidebottom et al.

Table 1 cont. Summary of siderophores identified using molecular networking and manual observations of the data. Nomenclature that are italicized were identified in this study.

	Name	Measured mass [M+H]+	Theoretical mass [M+H]+	Δ ppm	Sum formula [+H]+	ID confidence	Monoculture	Reference
DFO-Bs	*uC10 acyl DFO-B*	685.4856	685.4858	-0.29	$C_{34}H_{65}N_6O_8$	3		*This study*
	uC11 acyl DFO-B	699.5007	699.5025	-2.57	$C_{35}H_{69}N_6O_8$	3		*This study*
	C11 acyl-DFO	701.5174	701.5171	0.43	$C_{35}H_{69}N_6O_8$	2		Traxler et al; Sidebottom et al.
	C12 acyl-DFO	715.5322	715.5328	-0.84	$C_{36}H_{71}N_6O_8$	2		Traxler et al; Sidebottom et al.
	C13 acyl-DFO	729.5496	729.5484	1.64	$C_{37}H_{73}N_6O_8$	2		Traxler et al; Sidebottom et al.
	uC12 acyl FO-B [M+Al]+	737.4776	737.4752	3.25	$C_{36}H_{66}N_6O_8Al$	3		*This study*
	dodecanedioic DFO-B	745.5086	745.5070	2.15	$C_{36}H_{69}N_6O_{10}$	3		*This study*
	amphiphilic desferrioxamine 12	745.5438	745.5434	0.54	$C_{37}H_{73}N_6O_9$	2		Sidebottom et al.
	tridecanedioic DFO-B	759.5221	759.5226	-0.66	$C_{37}H_{71}N_6O_{10}$	3		*This study*
	amphiphilic desferrioxamine 15	759.5597	759.5590	0.92	$C_{38}H_{75}N_6O_9$	2		Sidebottom et al.
DFO-Ds	desferrioxamine H	461.2602	461.2606	-0.87	$C_{20}H_{37}N_4O_8$	2		Adapa et al.
	glutaric desferrioxamine H	475.2760	475.2762	-0.42	$C_{21}H_{39}N_4O_8$	2		*This study*
	C2 acyl glutaric desferrioxamine H	489.2900	489.2919	-3.88	$C_{22}H_{41}N_4O_8$	2		*This study*
	desferrioxamine D4	559.3453	559.3450	0.50	$C_{25}H_{47}N_6O_8$	2		*This study*
	deoxydesferrioxamine D3	587.3757	587.3763	-1.02	$C_{27}H_{51}N_6O_8$	3	*	*This study*
	Desferrioxamine D3	589.3915	589.3919	-0.68	$C_{27}H_{53}N_6O_8$	2	*	*This study*
	desferrioxamine D1	603.3714	603.3712	0.33	$C_{27}H_{51}N_6O_9$	2	*	
	C2 acyl DFO-D	617.3864	617.3869	-0.81	$C_{28}H_{53}N_6O_9$	2		*This study*
	C4 acyl DFO-D	645.4185	645.4182	0.46	$C_{30}H_{57}N_6O_9$	2	*	*This study*
	C5 acyl DFO-D	659.4331	659.4338	-1.06	$C_{31}H_{59}N_6O_9$	2		*This study*
	C6 acyl DFO-D	673.4498	673.4495	0.45	$C_{32}H_{61}N_6O_9$	2	*	*This study*
	C7 acyl DFO-D	687.4655	687.4651	0.58	$C_{33}H_{63}N_6O_9$	2	*	*This study*
	C11 acyl DFO-D	743.5280	743.5277	0.40	$C_{37}H_{71}N_6O_9$	2	*	*This study*
	C12 acyl DFO-D	757.5436	757.5434	0.26	$C_{38}H_{73}N_6O_9$	2	*	*This study*
	C13 acyl DFO-D	771.5607	771.5590	2.20	$C_{39}H_{75}N_6O_9$	2	*	*This study*
	C14 acyl DFO-D	785.5749	785.5747	0.25	$C_{40}H_{77}N_6O_9$	2	*	*This study*
tenacibactins	tenacibactin C	503.3070	503.3075	0.99	$C_{23}H_{43}N_4O_8$	3		Jang et al.
	tenacibactin E	531.3380	531.3388	-1.15	$C_{25}H_{47}N_4O_8$	3	*	*This study*
	tenacibactin F	545.3545	545.3545	0.00	$C_{26}H_{49}N_4O_8$	3	*	*This study*
	tenacibactin G	587.3990	587.4014	4.08	$C_{29}H_{55}N_4O_8$	3		*This study*
	tenacibactin H	601.4168	601.4171	-0.49	$C_{30}H_{57}N_4O_8$	3	*	*This study*
	tenacibactin I	615.4326	615.4327	-0.16	$C_{31}H_{59}N_4O_8$	3		*This study*
	tenacibactin J	629.4484	629.4484	0.00	$C_{32}H_{61}N_4O_8$	3		*This study*

191

192 **Acyl DFO production by *Streptomyces* sp. S29.** *Streptomyces* sp. S29 was able
193 to produce twelve new acyl DFO-Bs similar to those previously described.[26,27] Of these
194 12, five were short acyl chain derivatives (C_3, C_4, C_4 hydroxylated, C_5, and C_6), five were
195 monounsaturated derivatives (uC_6, uC_7, uC_{10}, uC_{11}, and uC_{12}), and two were derivatives
196 containing glutaric acid at the C-terminus, similar to those seen by Rütschlin et al.[40]
197 Pertaining to the unsaturated derivatives, placement of the alkene at the position α to the
198 carbonyl is based off previous studies also reporting DFOs containing unsaturated acyl
199 chains.[27,41] Additionally, the position of the hydroxy in the C_4 derivative was based on
200 previous work showing multiple amphiphilic peptide-based siderophores contain
201 hydroxylation at the β-position.[27,42]

202 We propose henceforth that the previously known 'acyl DFOs' should be renamed
203 'acyl DFO-B' due to the observation in this study of analogues that contain a *N*-acetyl-*N*-
204 hydroxycadaverine terminus, similar to desferrioxamine D. The new acyl DFO-D
205 analogues discovered here also range from short, medium and long acyl chained
206 derivatives (Table 1). It is likely the acyl DFOs are branched analogues as previous
207 studies noted that it was unlikely the chains were fully linear since *Streptomyces* spp.
208 utilise branched starter units in fatty acid synthesis.[26,27] This is also the case for the suite
209 of tenacibactin analogues observed in the data. These branched acyl chain siderophores
210 were originally observed in *Tenacibaculum* sp. A4K-17 [38], and are essentially truncated
211 versions of acyl DFO-Bs that lack the N-terminal *N*-hydroxycadaverine.

212 *Streptomyces coelicolor* has shown broad substrate specificity in regard to medium
213 and long acyl chain incorporation into desferrioxamine structures[19], but not short acyl
214 chained groups, where *Streptomyces* sp. S29 can facilitate production of short, medium,

215 and long acyl chained DFO-B analogues. Traxler et al. showed the ability of other
216 Actinobactera to react to the presence of *S. coelicolor*. through the production of acyl
217 DFO-B analogues.[26] Interestingly, we see this same phenomenon for the coculture of
218 *Streptomyces* sp. S29 and the fungi. Medium and long chained acyl DFO-Bs (including
219 unsaturated derivatives) were almost exclusively produced in coculture whereas short,
220 medium and long chained acyl DFO-Ds were produced under both mono- and coculture
221 conditions. The tenacibactin analogues were distributed amongst both cultures (Table 1).
222 It was hypothesized these long-chained derivatives might be a way for the uptake of these
223 analogues to bypass the DesE uptake mechanism, instead they 'hand-off' the Fe(III) via
224 membrane bound ferrioxamines.[19,43]

225 **Aryl DFO production by *Streptomyces* sp. S29.** The production of seven new
226 aryl DFOs related to legonoxamine A and B, which were also observed in this study (Table
227 1), shows the biosynthetic flexibility of *Streptomyces* sp. S29. These structures range
228 from being smaller, potential oligomers like legonoxamine C (*m/z* 351.1912, Figure S12)
229 to the larger legonoxamine H (*m/z* 665.3893, Figure S17). A few interesting legonoxamine
230 derivatives include legonoxamine F (Figure S15), putrescine-containing legonoxamine G
231 (Figure S15) and legonoxamine A glycoside (Figure S18).

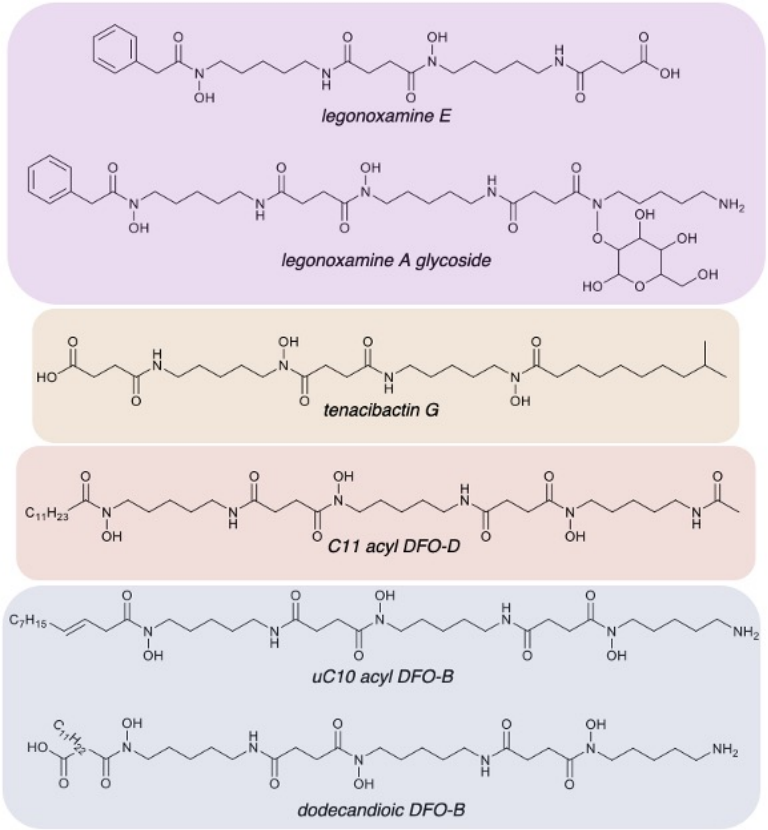

Figure 5. Representation of desferrioxamine structural diversity of *Streptomyces* sp. S29. (A-B) New legonoxamine derivatives (purple), tenacibactins (orange), DFO-Ds (red), and a variety of DFO-Bs (blue) were all found. Full MS/MS data and annotations can be found in supplementary for all 41 new analogues discovered.

232

233 Legonoxamine F contains one 1,6-diaminohexane instead of the typical 1,5-
234 diaminopentane. This is a well-established phenomenon in siderophore biosynthesis[31,44]
235 linking it to the promiscuity of the S29 *des* biosynthetic gene cluster. Legonoxamine G
236 contains a *N*-hydroxyputrescine moiety due to the initial loss of 104 Da instead of the
237 typical 118 Da associated to *N*-hydroxycadaverine. Putrebactin is the archetypal
238 putrescine containing siderophore[45], and as its biosynthetic gene cluster has been shown
239 to lack genes coding for production of putrescine, it is assumed that instead, this precursor
240 is sequestered from metabolite pools.[46] Interestingly, researchers have also found that
241 under putrescine-depleted conditions, *Shewanella putrefaciens* shifts to producing
242 desferrioxamine B when cadaverine precursors are available.[47] In desferrioxamine
243 biosynthesis, incorporation of the putrescine precursor in desferrioxamine A1 has been
244 shown before in multiple species[30,44,48] and now in this study with the discovery of
245 legonoxamine G.

246 Legonoxamine A glycoside was observed using the predicted molecular formula
247 ($C_{37}H_{62}N_6O_{13}$) and the loss of a sugar (-162 Da). An additional putative diglycosylated
248 DFO (*m/z* 899.4827), with a predicted molecular formula of $C_{38}H_{70}N_6O_{18}$, was observed
249 in the mass spectrum but upon selected ion monitoring (SIM), produced insufficient
250 fragment ions for structural characterisation. The production of glycosylated DFOs has
251 only been reported once before: nocardamin glucuronide, isolated from *Streptomyces* sp.
252 80H647.[49] There are only a few reports of microbial enzymes that produce glucuronides[50],
253 yet, the addition of glucose or other hexoses are more commonplace in bacterial natural
254 products. We propose legonoxamine A glycoside undergoes a similar glycosylation
255 mechanism to nocardamin glucuronide, occurring on a *N*-hydroxyl.

256 **Macrocyclised desferrioxamines**. We observe desferrioxamine E in the
257 molecular network (Figure S1) as well as several other macrocyclic DFOs. In Figure 3,
258 these are anchored by bisucaberin 01 (*m/z* 443), first described by Senges et al.[28] Based
259 on the molecular formulas, fragmentation patterns and the previously established
260 structure, we observe multiple additional macrocyclic derivatives connected via
261 bisucaberin 01 but their structures were not definable based on MS/MS data alone (Table
262 1). The putative macrocyclised derivatives extend by successive CH_2's , differing from the
263 study by Senges et al. which reduce in size, but the location of this extension requires
264 confirmation via NMR. Similar to acyl DFOs, macrocyclic derivatives have also shown to
265 have flexible biosynthesis in feeding studies, including the incorporation of 1,8-
266 diaminooctane moieties.[51] There was no observation of putrebactin, or avaroferrin in the
267 culture despite the similar biosynthesis with bisucaberins and desferrioxamines.

268 **Dicarboxylic acid desferrioxamine analogues.** Two new desferrioxamines,
269 observed only in coculture extracts, with dicarboxylic acid C-termini were also elucidated.
270 Dodecanedioic DFO-B (Figure S33) has an *m/z* of 745.5086, corresponding to the
271 molecular formula of $C_{36}H_{68}N_6O_{10}$. Tridecanedioic DFO-B (Figure S34) has an *m/z* of
272 759.5221, corresponding to the molecular formula of $C_{37}H_{70}N_6O_{10}$. This is the first
273 reported instance of large dicarboxylic acids being incorporated into DFO structures yet
274 there are examples of larger dicarboxylic acids being bound to CoA, like pimelic acid,
275 therefore we cannot rule the possibility out.

276 Microbial cytochrome p450s are responsible for adding complexity to fatty acids to
277 be used as building blocks for more complex metabolites or as signalling molecules.[52]
278 Previous studies have shown the bacterial production of dicarboxylic acids might occur

279 via cytochrome p450 monoxygenase.[53] In order to determine the presence of enzymes
280 that facilitate ω-oxidation in S29, protein sequences that belong to the long-chain fatty
281 acid ω-monooxygenase enzyme class (EC 1.14.14.80) and from fatty acid ω-oxidation
282 gene ontology (GO:0010430) were obtained from the Uniprot database. BLAST results
283 of these sequences against the S29 draft genome reveals just one hit (supplementary
284 data), comprising 3 orthologs with mid-term amino acid identity (40-50%), a methyl-
285 branched lipid ω-hydroxylase (cyp124) from Mycobacterium spp. (~43% identity) (Uniprot:
286 P9WPP2, P0A517 & P9WPP3). Pfam sequence search confirms cytochrome P450
287 domain for this protein and further experimentation could confirm its ω-monooxygenase
288 activity. Searching Uniprot under these search criteria returns only a handful of bacterial
289 sequences with a couple belonging to Actinobactera, therefore, the possibilities to track
290 this activity in the S29 genome are very narrow resulting in an inconclusive result
291 regarding the presence of an ω-monooxygenase in S29.

292 **Ferrioxamines and DFO presence in pure and coculture experiments.** A
293 number of metal complexed ferrioxamines were observed in subnetwork 2 (Figure 6).
294 Fe(III) and Al^{3+} are the only metals complexed with the variety of desferrioxamines
295 present, similar to studies before.[26,27] Although the binding affinity for Fe(III) is greater
296 than Al(III)[54], it appears that this difference in affinity is not enough to prevent Al(III)
297 chelation. The importance of iron has already been addressed in regard to bacteria and
298 cell maintenance but Al(III) is toxic and has no direct role in metabolism and seems to be
299 an consequence of the chemical ecology of these metabolites.

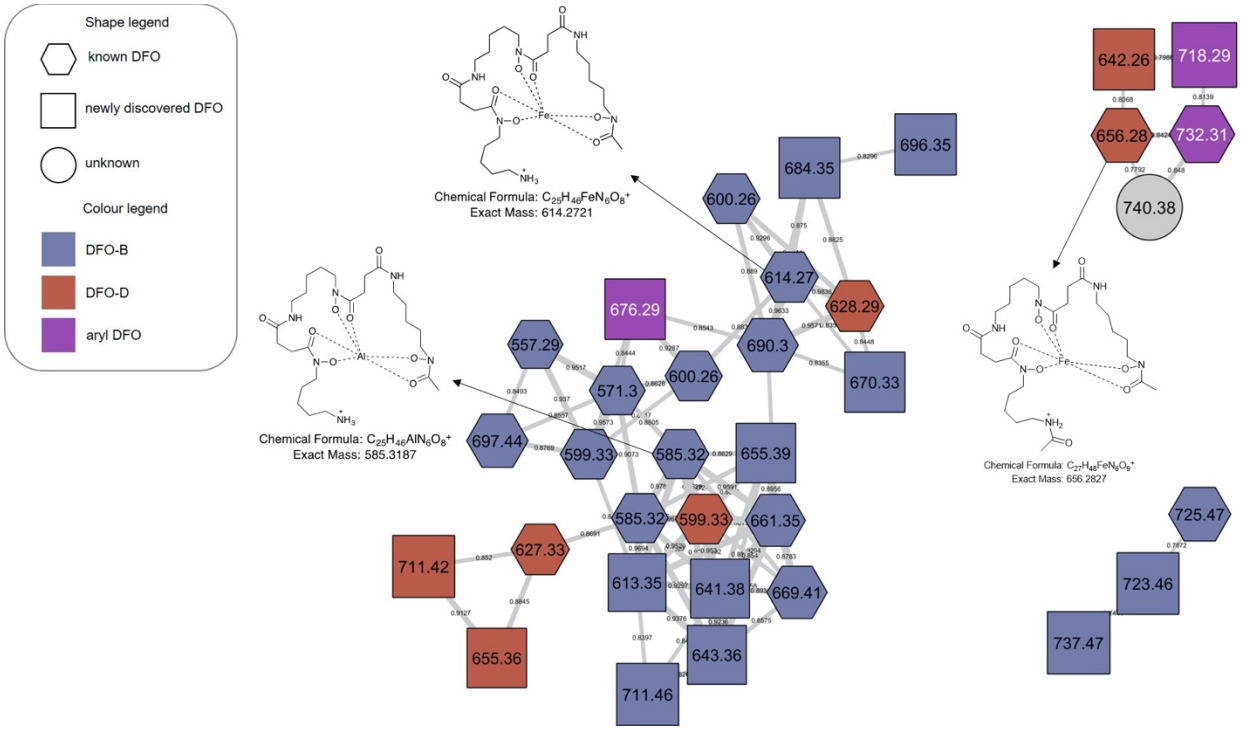

Figure 6. Metal-complexed molecular families. The GNPS library was able to identify multiple metal ion complexes (hexagonal nodes). All other features observed in the molecular network were assignable as Fe(III) or Al(III) bound ferrioxamines. Al(III) analogue of new desferrioxamine analogue –uC12 acyl FO-B. Table S1 contains accurate mass information on all complexed ions found in this figure.

The molecular network was also used to evaluate the production of the DFOs between the two cocultivations with *A. niger* and *B. cinerea* and the *Streptomyces* sp. S29 monoculture (Figure S3). The results showed that 32 of the 71 ions were present in the monoculture, whereas all of the remaining were found in coculture extracts only (Table 1). There was no qualitative significant difference in the siderophores produced under cocultivation with *A. niger* compared to those produced in cocultivation with *B. cinerea*, indicating the potential broad response to a fungal microbe in the environment. These results might point to DFO and siderophore production in a broader context as a common chemical response to other microbes, whether it be bacterial or fungal, in close environmental proximity to the primary organism.

311 **MS2LDA analysis.** In order to further evaluate the overall chemical space that
312 DFOs inhabit in the molecular network, MS2LDA was performed. MS2LDA is a technique
313 which identifies molecular 'fingerprints' in fragmentation patterns and assigns these into
314 motifs (13 Mass2Motifs were manually curated). By merging the two networks (GNPS
315 molecular network and MS2LDA) after motifs were annotated, it is clear that further DFO
316 chemical space is there to be discovered. Figure S4 represents the overall results of this
317 merged network where we have highlighted the previously identified features (107) and
318 edges (970) from the original molecular networking job and all of the nodes (351) and
319 edges (1991) that contain DFO motifs identified through MS2LDA. This near tripling of
320 features by inclusion of the MS2LDA workflow doesn't necessarily correlate to an
321 increase in metabolites, but upon validation of the data, there seems to be very minimal
322 features corresponding to isotopes or adducts.

323 In order to evaluate the accuracy of this analysis, a characterized DFO in this study
324 (legonoxamine E, Figure 5) and an unknown DFO observed using MS2LDA (*m/z* 650.37,
325 $[M+2H]^{2+}$) were more closely analysed (Figure S5). The unknown desferrioxamine is a
326 singleton (Figure S5B) in both the original network and the merged network, yet, MS2LDA
327 identifies it contains DFO motifs and upon closer inspection and prediction of its molecular
328 formula ($C_{59}H_{103}N_{12}O_{20}$). The potential of this putative DFO being a dimer was ruled out
329 based on fragmentation analysis lacking the monomer. Elucidation of its full structure was
330 not able to be completed with MS/MS data alone, therefore, further studies are underway
331 to characterise its structure. Nonetheless, this example displays the utility of MS2LDA to
332 evaluate the chemical potential of a bacterium and its potential use in these types of
333 studies in the future.

334 ***Streptomyces* sp. S29 siderophore biosynthetic gene clusters.** DFOs are
335 biosynthesized by nonribosomal peptide synthetase independent siderophore (NIS)
336 pathways and the presence of at least one gene encoding a homolog to IucA/IucC has
337 become recognized as a marker of NIS biosynthetic gene clusters.[55] DFO biosynthesis is
338 encoded by the highly conserved *des* biosynthetic gene cluster (*desEFABCD* genes)
339 found in many *Streptomyces* species [21]. Using FeGenie[56], the identification of iron-related
340 genes revealed 27 siderophore biosynthesis and 11 transport related genes in the
341 *Streptomyces* sp. S29 genome. These siderophore biosynthesis related genes are
342 grouped in five biosynthetic gene clusters and antiSMASH [57] predictions reveal that three
343 of the five contain at least one gene homolog to IucA/IucC and the other two correspond
344 to NRPS dependent pathways.

345 Region 7 (Figure S53) contains a siderophore BGC in *Streptomyces* sp. S29 with
346 high homology to *desA-D* genes and to the ferric-siderophore uptake and utilization genes
347 (*desE-F*). This *des* cluster follows the same structure as many *Streptomyces* spp.,
348 including the position of iron boxes upstream putative *desE* (s29_002291) and *desA*
349 (s29_002293) genes (Fig S31). DesC of the *des* BGC from *Streptomyces* sp. S29
350 (s29_2295) exhibits high identity to DesC from S. coelicolor (72%) and to LgoC from
351 *Streptomyces* sp. MA37 (69%). In *S. coelicolor* A3(2), transcription of *des* BGC is
352 repressed by the divalent metal-dependent regulatory (DmdR) protein DmdR1 and
353 derepressed by iron limitation.[58] BLASTN/P analysis revealed a putative DmdR repressor
354 in *Streptomyces* sp. S29 (s29_002782) with 89% nucleotide and 93% amino acid identity
355 to DmdR1 (AJ271797.1 / CAC28070.1). BLASTN analyses identified eight putative

356 DmdR-binding sites (iron boxes) in *Streptomyces* sp. S29 by query of putative iron boxes
357 found upstream in different ORFs in *S. coelicolor* A3(2) genome.[19]

358 Acyltransferases involved in hydroxamate biosynthesis normally exhibit narrow
359 substrate tolerance (e.g. IucB, which shows a high degree of specificity towards acetyl-
360 CoA).[19] The array of DFOs produced by *S. coelicolor* (B, E, G1 and amphiphilic) and aryl
361 DFOs (legonoxamine A-B) produced by *Streptomyces* sp. MA37, has been attributed to
362 substrate tolerant acyltransferases DesC and LgoC. [19,59] Senges et al. acknowledged in
363 their evaluation of the *Streptomyces chartreusis* secretome that in iron depleted minimal
364 medium they also observed additional desferrioxamines produced and that the overall
365 biosynthetic potential may be much broader than what has been predicted.[28] Cloning and
366 more detailed analysis of the *Streptomyces* sp. S29 *des* gene cluster is ongoing to link
367 the chemical potential shown in this study.

368 In conclusion, the chemistry observed in the *Streptomyces* sp. S29 secretome
369 shows it potential as an agent to prevent fungal infection, evidenced by its locking away
370 of Fe(III) via overproduction of desferrioxamines. New analogues were observed in both
371 monoculture and cocultivation studies with fungal phytopathogens, *A. niger* and *B.*
372 *cinerea*. *Streptomyces* sp. S29 seems to produce an arsenal of desferrioxamine
373 analogues using any available precursor materials available whether that be putrescine,
374 cadaverine, aryl, acyl, or long chained dicarboxylates. The role of bacterial communities
375 in plant and crop protection is becoming more important due to the growing world
376 population, with a strong emphasis on improving strategies at preventing phytopathogenic
377 infection. Overall, the production of 46 new and 25 previously reported siderophores

378 indicates this *Streptomyces* sp. should be studied further for its plant protective properties
379 as a biocontrol agent.

380 **EXPERIMENTAL SECTION**

381 *Strain collection*

382 *Streptomyces* sp. S29 was isolated from a soil sample collected from Lupine plant
383 (*Lupinus oreophilus*) roots originating from a polyextreme enviroment at Quebrada
384 Nacimiento, Socaire, San Pedro de Atacama, Atacama Desert (23°37'06''S;67°50'56''W
385 - 3,646 m.a.s.l). One aliquot was heated at 100 °C for 5 min and directly sprinkled onto
386 Gause #1 and Starch-Casein plates, both complemented with nystatin, cycloheximide
387 and nalidixic acid. Another aliquot was resuspended in ¼ Ringer solution, heated at 60
388 °C for 10 min and dilutions of $10^{-1/2}$ and 10^{-1} were spread onto agar plates. Plates were
389 incubated at 30 °C for ~1 week and colonies were subcultured on ISP2 plates. Based on
390 morphological characteristics of the colony and antifungal activity experiments against *B.*
391 *cinerea* and *A. niger*, 16S rRNA sequence of S29 isolate was used to identify and confirm
392 its taxonomy using EzBioCloud database (3) (data not shown).
393

394 *Phytopathogens*

395 *Aspergillus niger* and *Botrytis cinerea*, biochemically characterized field samples, were
396 provided by Laboratorio de microbiología, Facultad de Ciencias naturales, matemática y
397 medio ambiente, Universidad Tecnológica Metropolitana (UTEM), Santiago, Chile.
398 Molecular identification of these strains was carried out by sequencing of internal

399 transcribed spacer (ITS) region amplified by PCR using universal primers ITS1 and ITS4
400 (supplementary data).
401
402 *Biological screening*
403 Preliminary antifungal screening of the lupine rhizosphere *Streptomyces* collection was
404 carried out starting from spore stocks, where Streptomyces isolates were grown on ISP2
405 at 30°C for 1 week. On PDA plates, two inverted agar plugs (different isolates) from these
406 ISP2 plates, set at 2 cm from the centre, were grown at 30°C O.N. After this, the centre
407 of the PDA plates was inoculated using 10 μL of a $5x10^4$ spores/mL spore stock of a
408 phytopathogen (*Botrytis/Fusarium*) and grown at 25°C. Inhibition observations were
409 carried out at 4, 11 and 17 days from pathogen inoculation.
410 Disc diffusion assays were adapted for the microbes tested using the Clinical and
411 Laboratory Standards Institute M44 Method for Antifungal Disk Diffusion Susceptibility
412 Testing of Yeasts.[60] Extract concentrations were standardised to 200 μg/mL for all
413 bioassays conducted.
414 In order to conduct post-fermentation streaks, 50 μL of fermentation was
415 aseptically transferred onto a ISP2 agar plate. 24- and 48-hour incubation (28°C) intervals
416 were checked for fungal growth. Due to the faster growth rate of the fungi, we would
417 expect any presence of fungal spores to lead to the observation of mycelial growth, yet
418 no fungal growth was observed.

419 *Cocultivation and extraction*

420 A set of experiments were carried out on these three organisms in order to determine the
421 effect of the fungal culture being added to the *Streptomyces* sp. (a) *Streptomyces* sp. S29
422 alone: a single colony was aseptically transferred to 100 mL of iron deficient medium
423 (ISP2), shaken at room temperature at 150 RPM for 7 days, in order to induce production
424 of siderophores. (b) *Streptomyces* sp. S29 + *Aspergillus niger*: 100 mL of bacterial culture
425 was grown for 5 days, at room temperature and shaken at 150 RPM. On the second day
426 of bacterial growth, an independent axenic culture of *A. niger* (spores) was grown for 3
427 days (10 mL of PDA liquid medium, room temperature and 150 RPM shaking). On the
428 fifth day of bacterial growth, the fungal liquid culture was transferred axenically to the
429 bacterial culture and allowed to grow an addition 2 days. (c) *Streptomyces* sp. S29 +
430 *Botrytis cinerea*: the same procedure as described in experiment b was followed.
431 Additionally, each experiment contained 3 g/50 mL of sterilised glass beads to prevent
432 aggregation. Each coculture was then scaled up to 3 L total volume in an attempt to
433 produce sufficient secondary metabolites for structure elucidation.

434 Each liquid fermentation included Diaion HP-20 resin (3 g/50 mL) that was
435 sterilised with culture medium. After 7 days, the resin was vacuum filtered, subsequently
436 washed five times with milli-q water and finally macerated exhaustively in methanol (3×).
437 The methanolic extract was then dried on a rotary evaporator and subsequently
438 underwent Kupchan partitioning.[61] Finally, the *sec*-butanol fraction underwent C18 solid-
439 phase extraction (Phenomenex), with each separation yielding 5 fractions of increasing
440 methanol and these samples were subsequently prepared for LC-MS studies.

441 The 100% methanol fractions from the *Botrytis* and *Aspergillus* co-culture were
442 subjected to further separation via reversed phase-HPLC with a Waters Sunfire C18
443 semi-preparative column (5 μM, 100Å, 250 × 10 mm) wand a solvent system of A–95/5
444 MeOH/H_2O and B-MeOH. The Agilent 1200 HPLC utilized a solvent gradient of 0% B to
445 100% B at 2.0 mL/min over 50 min.

446 *Liquid chromatography – mass spectrometry*

447 All runs were analysed using an Agilent 1290 UHPLC coupled to Bruker MAXIS II Q-ToF
448 mass spectrometer. LC utilizes a Phenomenex Kinetex XB-C_{18} (2.6 mM, 100 × 2.1 mm)
449 column with a mobile phase of 5% MeCN+0.1% formic acid to 100% MeCN+0.1% formic
450 acid in 11 min. Bruker MAXIS II has a mass range of *m/z* 100-2000, capillary voltage 4.5
451 kV, nebulizer gas 5.0 bar, dry gas 12.0 l/min, and dry temperature of 220 °C. MS/MS
452 experiments were conducted under Auto MS/MS scan mode with a step collision energy
453 from 80-200%. Samples were prepared at a concentration of 0.3 mg/mL. Raw data files
454 were analysed using Bruker Daltonics 3.6.

455 *GNPS Molecular Networking and MS2LDA*

456 A molecular network was created using the online workflow (https://ccms-
457 ucsd.github.io/GNPSDocumentation/) on the GNPS website (http://gnps.ucsd.edu). The
458 data was filtered by removing all MS/MS fragment ions within +/- 17 Da of the precursor
459 m/z. MS/MS spectra were window filtered by choosing only the top 6 fragment ions in the
460 +/- 50Da window throughout the spectrum. The precursor ion mass tolerance was set to
461 0.02 Da and a MS/MS fragment ion tolerance of 0.02 Da. A network was then created
462 where edges were filtered to have a cosine score above 0.7 and more than 5 matched

463 peaks. Further, edges between two nodes were kept in the network if and only if each of
464 the nodes appeared in each other's respective top 10 most similar nodes. Finally, the
465 maximum size of a molecular family was set to 100, and the lowest scoring edges were
466 removed from molecular families until the molecular family size was below this threshold.
467 The spectra in the network were then searched against GNPS' spectral libraries. The
468 library spectra were filtered in the same manner as the input data. All matches kept
469 between network spectra and library spectra were required to have a score above 0.7
470 and at least 6 matched peaks. All features originating from the medium/instrument blanks
471 were excluded from the final molecular network.

472 For documentation on running MS2LDA, the user is referred to the original
473 publication and guidelines, which are also present at ms2lda.org.[62] All spectral images in
474 the supplementary information were created using Metabolomics Spectrum Resolver
475 (https://metabolomics-usi.ucsd.edu/).[63]

476 All siderophores dereplicated and elucidated in this study can be found in Table 1.
477 The structure elucidation of each new derivative and its corresponding MS/MS spectra
478 were generated using Metabolomics Spectrum Resolver are displayed in the
479 supplementary information (Table S2 and Figures S7-S52). All MS/MS spectra were also
480 annotated and deposited in the GNPS library, as well as the original datasets (Table S2).

481 **All data files and workflows can be found at the links below**:

482 GNPS molecular networking job:

483 https://gnps.ucsd.edu/ProteoSAFe/status.jsp?task=3c73305ef7ed48e19cb18e50b8b6b2bd

484 MS2LDA annotation experiment: http://ms2lda.org/basicviz/summary/1319/

485 MASSIVE: doi:10.25345/C5772V

486 *Streptomyces sp. S29 genome sequencing and assembly*

487 *Streptomyces* sp. S29 total DNA was extracted from liquid culture using DNeasy
488 UltraClean Microbial Kit (Qiagen). Whole genome sequencing (WGS) of the strain was
489 performed by an Illumina MiSeq (2 x 300 PE). Nanopore sequencing was performed using
490 a Rapid Sequencing Kit (SQK-RAD004) and MinIon Flow Cell (R9.4.1). The sequence
491 was assembled using Canu, polished using Racon, Illumina dataset was mapped onto
492 the contigs using BWA mem and then corrected using Pilon. The genome was annotated
493 using NCBI pgap software (6).

494

495 **ASSOCIATED CONTENT**

496 **Supplementary Information**

497 Tables of known and new desferrioxamine derivatives and their corresponding CCMS
498 Library IDs and Metabolomics Resolver Images (Table S2), disc diffusion assay results,
499 desferrioxamine containing subnetworks, new desferrioxamine analogues with annotated
500 structures and MS^2 spectra, ITS regions for fungal phytopathogens, cytochrome p450
501 enzyme sequence.

502 **Author Contributions**

503 DLS† and ED† contributed equally to this work.

504 **Conflicts of interest**

505 There are no conflicts of interest to declare.

506 **Acknowledgements**

507 SAJ would like to thank the University of Aberdeen for funding doctoral studies through
508 and Elphinstone Scholarship. DL would like to thank the Agencia Nacional de

Investigación y Desarrollo (ANID) for funding doctoral studies through 'Beca nacional de doctorado' Scholarship. ED would like to thank the Ministry of Higher Education and Scientific Research - Sudan, together with the University of Khartoum, for joint funding of master's studies. We would like to thank to Valeria Razmilic and Jean Franco Castro for their valuable advice and work in the setup of Lupine *Streptomyces* culture collection. We would also like to thank the support team at GNPS and Justin J.J. van der Hooft at MS2LDA for help with data deposition and for help at any stage of running the relevant workflows.

References

1 R. G. Expósito, I. de Bruijn, J. Postma and J. M. Raaijmakers, *Frontiers in Microbiology*, 2017, **8**, DOI:10.3389/fmicb.2017.02529.

2 O. S. Olanrewaju and O. O. Babalola, *Applied Microbiology and Biotechnology*, 2019, **103**, 1179–1188.

3 Y. Goudjal, O. Toumatia, N. Sabaou, M. Barakate, F. Mathieu and A. Zitouni, *World Journal of Microbiology and Biotechnology*, 2013, **29**, 1821–1829.

4 S. E. Jones and M. A. Elliot, *Trends in Microbiology*, 2017, **25**, 522–531.

5 V. C. Verma, S. K. Singh and S. Prakash, *Journal of Basic Microbiology*, 2011, **51**, 550–556.

6 A. Ciancio, C. M. J. Pieterse and J. Mercado-Blanco, *Frontiers in Microbiology*, 2016, **7**, DOI:10.3389/fmicb.2016.01620

7 J. M. Whipps, *Journal of Experimental Botany*, 2001, **52**, 487–511.

8 J. Shafi, H. Tian and M. Ji, *Biotechnology and Biotechnological Equipment*, 2017, **31**, 446–459.

9 D. M. Weller, in *Phytopathology*, 2007, **97**, 250–256.

10 Z. R. Suárez-Moreno, D. M. Vinchira-Villarraga, D. I. Vergara-Morales, L. Castellanos, F. A. Ramos, C. Guarnaccia, G. Degrassi, V. Venturi and N. Moreno-Sarmiento, *Frontiers in Microbiology*, 2019, **10**, DOI:10.3389/fmicb.2019.00290.

11 H. Idris, M. Goodfellow, R. Sanderson, J. A. Asenjo and A. T. Bull, *Scientific Reports*, 2017, **7,** DOI:10.1038/s41598-017-08937-4.

12 ODEPA - Oficina de Estudios y Políticas Agrarias, Vinos, https://www.odepa.gob.cl/rubros/vinos-y-alcoholes, (accessed May 26, 2020).

13 M. Sandy and A. Butler, *Chemical Reviews*, 2009, **109**, 4580–4595.

14 J. Kramer, Ö. Özkaya and R. Kümmerli, *Nature Reviews Microbiology*, 2020, **18**, 152–163.

15 R. Saha, N. Saha, R. S. Donofrio and L. L. Bestervelt, *Journal of Basic Microbiology*, 2013, **53**, 303–317.

16 B. Casentini and M. Pettine, *Applied Geochemistry*, 2010, **25**, 1688–1698.
17 K. E. Jones, K. L. Batchler, C. Zalouk and A. M. Valentine, *Inorganic Chemistry*, 2017, **56**, 1264–1272.
18 U. Neubauer, G. Furrer and R. Schulin, *European Journal of Soil Science*, 2002, **53**, 45–55.
19 J. L. Ronan, N. Kadi, S. A. McMahon, J. H. Naismith, L. M. Alkhalaf and G. L. Challis, *Philosophical Transactions of the Royal Society B: Biological Sciences*, 2018, **373**, DOI:10.1098/rstb.2017.0068.
20 T. Schupp, U. Waldmeier and M. Divers, *FEMS Microbiology Letters*, 1987, **42**, 135–139.
21 F. Barona-Gómez, U. Wong, A. E. Giannakopulos, P. J. Derrick and G. L. Challis, *Journal of the American Chemical Society*, 2004, **126**, 16282–16283.
22 A. D'Onofrio, J. M. Crawford, E. J. Stewart, K. Witt, E. Gavrish, S. Epstein, J. Clardy and K. Lewis, *Chemistry and Biology*, 2010, **17**, 254–264.
23 F. Maglangit, M. H. Tong, M. Jaspars, K. Kyeremeh and H. Deng, *Tetrahedron Letters*, 2019, **60**, 75–79.
24 R. D. Firn and C. G. Jones, *Natural Product Reports*, 2003, **20**, 382–391.
25 T. Pluháček, K. Lemr, D. Ghosh, D. Milde, J. Novák and V. Havlíček, *Mass Spectrometry Reviews*, 2016, **35**, 35–47.
26 M. F. Traxler, J. D. Watrous, T. Alexandrov, P. C. Dorrestein and R. Kolter, *mBio*, 2013, **4**, DOI:10.1128/mBio.00459-13.
27 A. M. Sidebottom, A. R. Johnson, J. A. Karty, D. J. Trader and E. E. Carlson, *ACS Chemical Biology*, 2013, **8**, 2009–2016.
28 C. H. R. Senges, A. Al-Dilaimi, D. H. Marchbank, D. Wibberg, A. Winkler, B. Haltli, M. Nowrousian, J. Kalinowski, R. G. Kerr and J. E. Bandow, *Proceedings of the National Academy of Sciences of the United States of America*, 2018, **115**, 2490–2495.
29 W. J. Moree, V. v. Phelan, C. H. Wu, N. Bandeira, D. S. Cornett, B. M. Duggan and P. C. Dorrestein, *Proceedings of the National Academy of Sciences of the United States of America*, 2012, **109**, 13811–13816.
30 T. J. Telfer, M. P. Gotsbacher, C. Z. Soe and R. Codd, *ACS Chemical Biology*, 2016, **11**, 1452–1462.
31 N. Ejje, C. Z. Soe, J. Gu and R. Codd, in *Metallomics*, 2013, **5**, 1519–1528.
32 M. Wang, J. J. Carver, V. v. Phelan, L. M. Sanchez, N. Garg, Y. Peng, D. D. Nguyen, J. Watrous, C. A. Kapono, T. Luzzatto-Knaan, C. Porto, A. Bouslimani, A. v. Melnik, M. J. Meehan, W. T. Liu, M. Crüsemann, P. D. Boudreau, E. Esquenazi, M. Sandoval-Calderón, R. D. Kersten, L. A. Pace, R. A. Quinn, K. R. Duncan, C. C. Hsu, D. J. Floros, R. G. Gavilan, K. Kleigrewe, T. Northen, R. J. Dutton, D. Parrot, E. E. Carlson, B. Aigle, C. F. Michelsen, L. Jelsbak, C. Sohlenkamp, P. Pevzner, A. Edlund, J. McLean, J. Piel, B. T. Murphy, L. Gerwick, C. C. Liaw, Y. L. Yang, H. U. Humpf, M. Maansson, R. A. Keyzers, A. C. Sims, A. R. Johnson, A. M. Sidebottom, B. E. Sedio, A. Klitgaard, C. B. Larson, C. A. P. Boya, D. Torres-Mendoza, D. J. Gonzalez, D. B. Silva, L. M. Marques, D. P. Demarque, E. Pociute, E. C. O'Neill, E. Briand, E. J. N. Helfrich, E. A. Granatosky, E. Glukhov, F. Ryffel, H. Houson, H. Mohimani, J. J.

Kharbush, Y. Zeng, J. A. Vorholt, K. L. Kurita, P. Charusanti, K. L. McPhail, K. F. Nielsen, L. Vuong, M. Elfeki, M. F. Traxler, N. Engene, N. Koyama, O. B. Vining, R. Baric, R. R. Silva, S. J. Mascuch, S. Tomasi, S. Jenkins, V. Macherla, T. Hoffman, V. Agarwal, P. G. Williams, J. Dai, R. Neupane, J. Gurr, A. M. C. Rodríguez, A. Lamsa, C. Zhang, K. Dorrestein, B. M. Duggan, J. Almaliti, P. M. Allard, P. Phapale, L. F. Nothias, T. Alexandrov, M. Litaudon, J. L. Wolfender, J. E. Kyle, T. O. Metz, T. Peryea, D. T. Nguyen, D. VanLeer, P. Shinn, A. Jadhav, R. Müller, K. M. Waters, W. Shi, X. Liu, L. Zhang, R. Knight, P. R. Jensen, B. Palsson, K. Pogliano, R. G. Linington, M. Gutiérrez, N. P. Lopes, W. H. Gerwick, B. S. Moore, P. C. Dorrestein and N. Bandeira, *Nature Biotechnology*, 2016, **34**, 828–837.

33 B. D. Corbin, E. H. Seeley, A. Raab, J. Feldmann, M. R. Miller, V. J. Torres, K. L. Anderson, B. M. Dattilo, P. M. Dunman, R. Gerads, R. M. Caprioli, W. Nacken, W. J. Chazin and E. P. Skaar, *Science*, 2008, **319**, 962–965.

34 M. G. Thompson, B. W. Corey, Y. Si, D. W. Craft and D. v. Zurawski, *Antimicrobial Agents and Chemotherapy*, 2012, **56**, 5419–5421.

35 J. L. Cleary, S. Kolachina, B. E. Wolfe and L. M. Sanchez, *mSystems*, 2018, **3**, DOI:10.1128/msystems.00036-18.

36 P. A. G. Elmer and T. Reglinski, *Plant Pathology*, 2006, **55**, 155–177.

37 G. Perrone, A. Susca, G. Cozzi, K. Ehrlich, J. Varga, J. C. Frisvad, M. Meijer, P. Noonim, W. Mahakamchanakul and R. A. Samson, in *Studies in Mycology*, Centraalbureau voor Schimmelculturen, 2007, **59**, 53–66.

38 J. H. Jang, K. Kanoh, K. Adachi, S. Matsuda and Y. Shizuri, *Journal of Natural Products*, 2007, **70**, 563–566.

39 E. L. Schymanski, J. Jeon, R. Gulde, K. Fenner, M. Ruff, H. P. Singer and J. Hollender, *Environmental Science and Technology*, 2014, **48**, 2097–2098.

40 S. Rütschlin and T. Böttcher, *Chemistry - A European Journal*, 2018, **24**, 16044–16051.

41 M. Luo, E. A. Fadeev and J. T. Groves, *Journal of the American Chemical Society*, 2005, **127**, 1726–1736.

42 J. D. Martin, A. E. Yusai, I. Ae, V. v Homann, M. G. H. Ae and A. Butler, *Journal of Biological Inorganic Chemistry*, 2007, **12**, 461–475.

43 J. S. Martinez, G. P. Zhang, P. D. Holt, H. T. Jung, C. J. Carrano, M. G. Haygood and A. Butler, *Science*, 2000, **287**, 1245–1247.

44 M. P. Gotsbacher and R. Codd, *ChemBioChem*, 2020, **21**, 1433–1445.

45 K. M. Ledyard, A. Butler, K. M. Ledyard and A. Butler, *Structure of putrebactin, a new dihydroxamate siderophore produced by Shewanella putrefaciens*, 1997, **2**, 93-97.

46 C. Z. Soe, A. A. H. Pakchung and R. Codd, *Chemistry & Biodiversity*, 2012, **9**, 1880–1890.

47 S. Rütschlin, S. Gunesch and T. Böttcher, *Cell Chemical Biology*, 2017, **24**, 598-604.e10.

48 R. C. Hider and X. Kong, *Natural Product Reports*, 2010, **27**, 637–657.

49 J. A. v. Lopez, T. Nogawa, Y. Futamura, T. Shimizu and H. Osada, *Journal of Antibiotics*, 2019, **72**, 991–995.

50 S. I. Elshahawi, K. A. Shaaban, M. K. Kharel and J. S. Thorson, *Chemical Society Reviews*, 2015, **44**, 7591–7697.

51 J. Meiwes, H.-P. Fiedler, H. Zähner, S. Konetschny-Rapp and G. Jung, *Production of desferrioxamine E and new analogues by directed fermentation and feeding fermentation*, 1990, **32**, 505-510.

52 I. N. A. van Bogaert, S. Groeneboer, K. Saerens and W. Soetaert, *FEBS Journal*, 2011, **278**, 206–221.

53 S. Honda Malca, D. Scheps, L. Kühnel, E. Venegas-Venegas, A. Seifert, B. M. Nestl and B. Hauer, *Chemical Communications*, 2012, **48**, 5115–5117.

54 G. Anderegg, F. L'Eplattenier and G. Schwarzenbach, *Helvetica Chimica Acta*, 1963, **46**, 1400–1408.

55 G. L. Challis, *ChemBioChem*, 2005, **6**, 601–611.

56 A. I. Garber, K. H. Nealson, A. Okamoto, S. M. McAllister, C. S. Chan, R. A. Barco and N. Merino, *Frontiers in Microbiology*, 2020, **11**, 37.

57 K. Blin, S. Shaw, K. Steinke, R. Villebro, N. Ziemert, S. Y. Lee, M. H. Medema and T. Weber, *Nucleic acids research*, 2019, **47**, W81–W87.

58 F. J. Flores and J. F. Martín, *Biochemical Journal*, 2004, **380**, 497–503.

59 F. M. Maglangit, S. Alrashdi, J. Renault, L. Trembleau, C. Victoria, M. H. Tong, S. Wang, K. Kyeremeh and H. Deng, *Organic & Biomolecular Chemistry*, 2020, **18**, 2219-2222.

60 *M44 : method for antifungal disk diffusion susceptibility testing of yeasts, 3rd edition.*, NIELSEN BOOKDATA, 2018.

61 M. Houssen,W. and Jaspars, in *Natural Products Isolation*, ed. A. Sarker, S.; Latfi, Z.; Gray, Humana Press, Second., 2006, p. 380.

62 J. J. J. van der Hooft, J. Wandy, M. P. Barrett, K. E. V. Burgess and S. Rogers, *Proceedings of the National Academy of Sciences of the United States of America*, 2016, **113**, 13738–13743.

63 M. Wang, S. Rogers, W. Bittremieux, C. Chen, P. C. Dorrestein, E. L. Schymanski, T. Schulze, S. Neumann and R. Meier, *bioRxiv*, 2020, 2020.05.09.086066.